ISSN 1590-8844
International Journal of Mechanics and Control, Vol. 17, No. 01, 2016

CLOSING SEQUENCE OF AN UNDERACTUATED ANTHROPOMORPHIC MECHANICAL FINGER

Francesco Penta

Università degli Studi di Napoli Federico II, Dipartimento di Ingegneria Industriale

ABSTRACT

The mechanical behavior of an under-actuated finger device equipped with only one flexural tendon and only one extensor tendon is studied. The finger equilibrium is analyzed by an energetic approach; this permitted to identify some preliminary design criteria useful to obtain both the regularity of the finger motion and a human like closure sequence. Furthermore, a sufficient condition for the stability of the finger equilibrium is also derived. In the paper some numerical data to be used as starting point for any finger design purpose are also reported. To substantiate the proposed criteria, numerical results obtained from a finger case study are finally presented and discussed.

Keywords: Mechanical finger, finger design criteria, finger buckling, anthropomorphic closing sequence

1 INTRODUCTION

Since long time for the construction of robotic grasping devices and human hand prosthesis, the principles of under-actuation are adopted. This because by this approach, the number of servomotors or servo-actuators are greatly reduced and the control architectures are also simplified [1-13]. However, under-actuation make crucial the analysis and design of the main components of these devices, i.e. the fingers. If, actually, in the finger equilibrium paths unstable configurations are present, device control become impossible and, consequently, the grasping forces may reduce to unsatisfying levels. A second feature that also has to be examined with particular care is the sequence of relative rotations between the phalanxes by which the finger encloses the object to be grasped [14-19]. It is quite evident that if the closing sequence is incorrect the grasping action may become precarious or unstable or even the finger may close on itself without grasping. At present, the design of an under-actuated finger is carried out by trial and error on the base of results obtained by numerical models or direct experimentation on finger prototypes.

Contact author: Francesco Penta

Address: P.le V. Tecchio n° 80 – 80125 Naples – Italy
Phone: +39 – (0)81 7682451
E-mail: penta@unina.it

The high number of geometrical parameters on which the mechanical behaviour of an under-actuated finger depends and the analytical difficulties that are encountered when the stiffness matrix of the device is analysed make practically impossible the use of a direct method to identify the optimal geometry of its joints. In the present paper for the special case of an under-actuated finger equipped with double tendon (one for the flexion, the other for the finger extension) an approximated method is presented to optimize the geometry of the tendon guides of both the tendons. The study is based on some theoretical and experimental results obtained in previous works [7, 20-21]. Firstly, a sufficient condition for the stability of the finger equilibrium is given. Then, preliminary design criteria for the regularity of the finger motion and an anthropomorphic closure sequence are also obtained. Finally, to substantiate the proposed methods, some numerical examples are presented and discussed.

2 THE FINGER MECHANICAL MODEL

A schematic sketch of the finger device analysed in the present study is given in fig. 1. The finger is composed of four rigid links jointed by means of three hinges free of friction. Of these four links, one is fixed since it acts as metacarpal phalanx; the remaining three are movable and function as proximal, medial and distal phalanxes. The flexor and extensor moments are applied to each phalanx thanks to a couple of tendons having an end fixed to the distal phalanx.

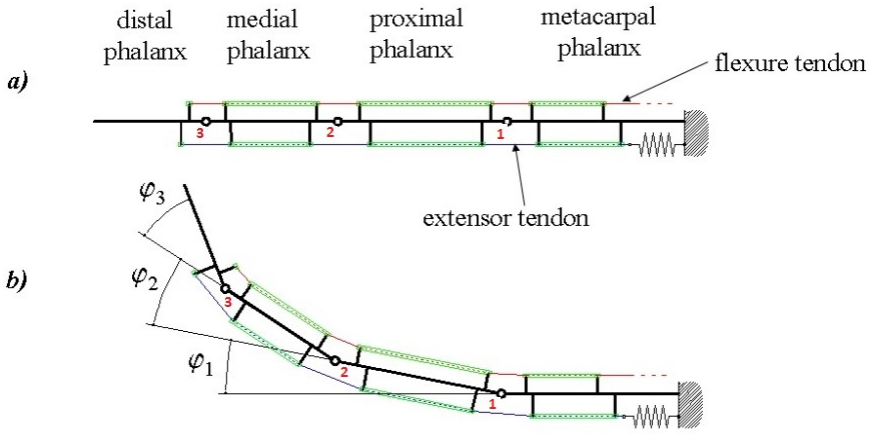

Figure 1 Scheme of the finger; initial or extended configuration (a) and deformed or bent configuration (b). Adapted from [21].

The extensor tendon is also elastically constrained to the metacarpal phalanx by a spring which stiffness is *k*. To the free end of the flexural tendon, instead an actuator applies the traction force causing the finger deformation. All the phalanxes, furthermore, are provided with a couple of cylindrical guides where the tendons can freely slide when the finger phalanxes rotate. We assume that both tendons are inextensible, have negligible thickness and negligible bending stiffness.

As lagrangian coordinates of the finger the absolute rotation φ_1 of its proximal phalanx, the relative rotation φ_2 between the proximal and the medial phalanx and, finally, the relative rotation φ_3 between the medial and the distal phalanx were considered (Fig. 2b). Hence, a finger configuration is univocally defined by the vector column $\boldsymbol{\varphi} = \left[\varphi_1, \varphi_2, \varphi_3\right]^T$.

In the present study the initial or reference configuration of the finger is the one with all the phalanxes totally extended (see Fig. 2-a)), that is with all the rotations $\varphi_i = 0,$ with $i = 1,2,3$. For sake of simplicity, the hinges of the finger are numbered consistently with the notation adopted for the lagrangian coordinates: *i* will denote the hinge where the rotation φ_i occurs.

Moreover, a movable phalanx is also identified by the same number of the hinge that is on its right side in the reference configuration.

The parameters that define the geometry of the tendons close to the *i*-th joint or hinge are shown in the enlarged view of fig. 2. The length z_i of the free-path P_iQ_i followed by the flexural tendon and the length l_i of the free path R_iS_i of the extensor tendon can be expressed as:

$$\begin{aligned} z_i &= \sqrt{s_i^2 + d_i^2 - 2 s_i d_i \cos\left(\Phi_i - \varphi_i\right)} = s_i \cdot \zeta_i\left(\varphi_i\right) \\ l_i &= \sqrt{\bar{s}_i^2 + \bar{d}_i^2 - 2 \bar{s}_i \bar{d}_i \cos\left(\bar{\Phi}_i + \varphi_i\right)} = \bar{s}_i \cdot \lambda_i\left(\varphi_i\right), \end{aligned} \tag{1}$$

$\zeta_i = \sqrt{1 + \varepsilon_i^2 - 2\varepsilon_i \cos\left(\Phi_i - \varphi_i\right)}$ and $\lambda_i = \sqrt{1 + \bar{\varepsilon}_i^2 - 2\bar{\varepsilon}_i \cos\left(\bar{\Phi}_i - \varphi_i\right)}$ are non-dimensional functions of the relative rotation φ_i, that depend respectively also on the non-dimensional ratios $\varepsilon_i = \dfrac{d_i}{s_i}$ and $\bar{\varepsilon}_i = \dfrac{\bar{d}_i}{\bar{s}_i}$ defining the initial shape of the joint.

The distances b_i and $\bar{b}_i$ of fig. 2, that separate the free-paths respectively of the flexor and extensor tendons from the hinge center O_i, are given by:

$$\begin{aligned} b_i &= -\frac{dz_i}{d\varphi_i} = s_i \cdot \beta_i\left(\varphi_i\right), \\ \bar{b}_i &= \frac{dl_i}{d\varphi_i} = \bar{s}_i \cdot \bar{\beta}_i\left(\varphi_i\right), \end{aligned} \tag{2}$$

where:

$$\begin{aligned} \beta_i &:= \frac{\varepsilon_i \sin\left(\Phi_i - \varphi_i\right)}{\sqrt{1 + \varepsilon_i^2 - 2\varepsilon_i \cos\left(\Phi_i - \varphi_i\right)}}, \\ \bar{\beta}_i &:= \frac{\bar{\varepsilon}_i \sin\left(\bar{\Phi}_i + \varphi_i\right)}{\sqrt{1 + \bar{\varepsilon}_i^2 - 2\bar{\varepsilon}_i \cos\left(\bar{\Phi} + \varphi_i\right)}}. \end{aligned} \tag{3}$$

When the finger, starting from its reference configuration reaches the configuration $\boldsymbol{\varphi}$, the flexor tendon free paths $P_i\bar{Q}_i$ experience the shortenings

$$\Delta z_i = z_{0i} - z_i, \; i = 1,2,3; \tag{4}$$

with z_{0i} initial value of z_i (Fig. 2-a). Consequently, the free end of the flexor tendon performs the displacement u given by:

$$u = \sum_{i=1}^{3} \Delta z_i \tag{5}$$

Similarly, the elongation Δl of the spring constraining the extensor tendon to the metacarpal phalanx is:

$$\Delta l = \sum_{i=1}^{3} \bar{s}_i \left[\lambda_i\left(\varphi_i\right) - \lambda_{i0}\right] \tag{6}$$

with $\lambda_{i0} = \lambda_i(0) = \sqrt{1 + \bar{\varepsilon}_i^2 + 2\bar{\varepsilon}_i \cos\left(\bar{\Phi}\right)}$ initial value of λ.

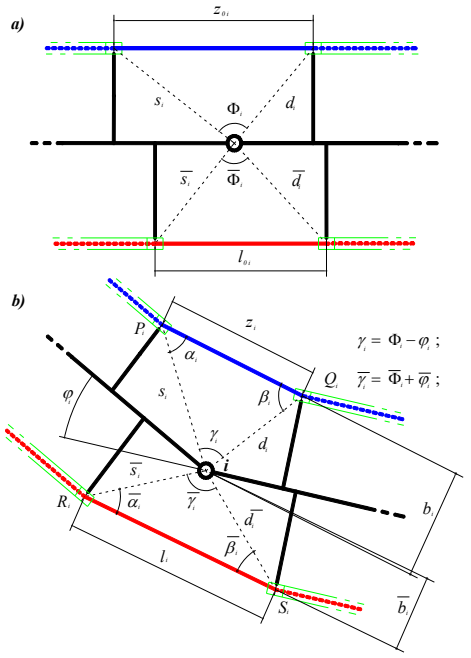

Figure 2 Initial (a) and deformed (b) configurations of the i-th joint. Adapted from [21].

As to the effects of the shape parameter ε_i on the mechanical behaviour of the finger, we observe preliminary that the function $z_i(\varphi_i)$ and its derivatives are invariant when the values of the distances s_i and d_i of fig. 2 are exchanged. This means that a joint where:

$$s_i = \overline{s} \text{ and } d_i = \varepsilon_i^* s_i, \text{ with } \varepsilon_i^* > 1, \tag{7}$$

has the same behaviour as the one with:

$$s_i = \varepsilon_i^* \overline{s} \text{ and } d_i = \overline{s} = \hat{\varepsilon}_i^* s_i \text{ with } \hat{\varepsilon}_i^* = \frac{1}{\varepsilon_i^*} < 1. \tag{8}$$

For this reason in the present study only joints with $\varepsilon_i \in [0,1]$ will be considered. Similar considerations apply for the effects of the other shape parameter $\overline{\varepsilon}_i$ and the function $\lambda_i(\varphi_i)$. Regardless of the effective shapes and sizes of the external surfaces of the phalanxes (where the contact with the objects to be grasped or with the other phalanxes takes place), we assume in the following that the range of values in which each rotation φ_i may vary has the angle Φ_i of fig. 2-a) as upper end, namely $\varphi_i \in [0, \Phi_i]$.

2.1 THE FINGER EQUILIBRIUM EQUATIONS

Under the stated hypothesis, the finger under the action of the horizontal load f applied to the flexural tendon is a conservative system. Hence, its equilibrium configuration $\boldsymbol{\varphi}$ has to satisfy the stationary condition of the total potential energy E, that is:

$$\begin{aligned} dE &= d\left(\frac{1}{2}k \cdot \Delta l^2 - f \cdot u\right) \\ &= \frac{\partial}{\partial \varphi_i}\left(\frac{1}{2}k \cdot \Delta l^2 - f \cdot u\right) d\varphi_i = 0 \qquad \forall d\varphi_i. \end{aligned} \tag{9}$$

Carrying out differentiation in eq. (9) and taking account of eq.(1) – (6), the set of equilibrium conditions is derived:

$$k\Delta l \cdot \overline{b}_i = f\, b_i, \qquad i = 1, 2, 3. \tag{10}$$

By equating the expressions of the load f obtained from each of equations (10) and simplifying the common factors, then the following chain of equalities is obtained:

$$\alpha_1 \frac{\overline{\beta}_1(\varphi_1)}{\beta_1(\varphi_1)} = \alpha_2 \frac{\overline{\beta}_2(\varphi_2)}{\beta_2(\varphi_2)} = \alpha_3 \frac{\overline{\beta}_3(\varphi_3)}{\beta_3(\varphi_3)}; \tag{11}$$

According to previous result, the finger equilibrium configurations are only those for which the three arm ratios $r_i = \alpha_i \cdot \left(\overline{\beta}_i / \beta_i\right)$ are equal. In order to the finger leaves the reference or initial configuration without significant vibrations or other dynamic effects when the load f is gradually applied to the flexor tendon, it is necessary that:

$$\rho_1(0) = \rho_2(0) = \rho_3(0). \tag{12}$$

These particular conditions can be met by several choices of the geometrical parameters of the finger joints. Among them, the one offering the possibility of obtain a quite wide set of finger closure sequences consists of choosing the angles $\Phi_i = 0$, since it will result:

$$\rho_i(0) = 0 \tag{13}$$

for any value of the shape parameters ε_i and $\varepsilon_i^{(e)}$ as well of the non-dimensional parameters α_i.

2.2 A CONDITION FOR THE FINGER STABILITY

To analyse the properties of the finger equilibrium configurations, the second variation d_2E of the potential E has to be considered. This latter is given by:

$$d_2E = \frac{\partial}{\partial \varphi_j}\left(k\Delta l\, \overline{b}_i - f\, b_i\right) d\varphi_i\, d\varphi_j \tag{14}$$

Since the total differential of Δl has the following expression:

$$d\Delta l = \frac{\partial \Delta l}{\partial \varphi_k} d\varphi_k = \overline{b}_k\, d\varphi_k \tag{15}$$

and observing that

$$\begin{aligned} &\frac{\partial}{\partial \varphi_j}\overline{b}_i(\varphi_i) = \delta_{ij}\overline{b}_i'(\varphi_i) \\ &\frac{\partial}{\partial \varphi_j} b_i(\varphi_i) = \delta_{ij} b_i'(\varphi_i), \end{aligned} \tag{16}$$

the second variation d_2E can also be written in the form:

$$\begin{aligned} d_2E &= k\left(d\Delta l\right)\overline{b}_i\, d\varphi_i + \left(k\Delta l\, \overline{b}_i' - f\, b_i'\right) d\varphi_i^2 = \\ &= k\left(d\Delta l\right)^2 + k\Delta l\, \overline{b}_i \left(\frac{\overline{b}_i'}{\overline{b}_i} - \frac{b_i'}{b_i}\right) d\varphi_i^2, \end{aligned} \tag{17}$$

where the last equality is obtained by substituting the expression $f = k\Delta l\left(\overline{b}_i / b_i\right)$ derived from equilibrium equations (10).

By eq. (17) it is immediately recognized that a sufficient condition for stability of finger equilibrium is:

$$\frac{\bar{b}_i'}{\bar{b}_i}-\frac{b_i'}{b_i}=\frac{\bar{\beta}_i'}{\bar{\beta}_i}-\frac{\beta_i'}{\beta_i}>0 \quad \forall \varphi_i \in [0,\Phi_i]. \tag{18}$$

As shown by the results of fig. 3, where the quantities $\bar{\beta}_i'/\bar{\beta}_i$ and β_i'/β_i are diagrammed as function of the relative rotations φ_i for $\bar{\Phi}_i=0$ and for the two cases of particular interest for the practical applications, namely $\Phi_i=\pi/2$ and $\Phi_i=2\pi/3$, for any value of the shape ratio ε_i the condition (18) can be satisfied choosing $\bar{\varepsilon}_i$ lesser than the limit value $\bar{\varepsilon}_{\lim}$. This particular value of $\bar{\varepsilon}_i$ depends on ε_i since it makes the $\bar{\beta}_i'/\bar{\beta}_i$ curve as function of φ_i tangent to the analogous β_i'/β_i curve. In the diagram of fig. 4, the curve of $\bar{\varepsilon}_{\lim}$ as function of ε_i are traced. They were obtained numerically solving, for each value of ε_i, the following system of algebraic equations:

$$\begin{cases} \dfrac{\beta'}{\beta}=\dfrac{\bar{\beta}'}{\bar{\beta}}, \\ \dfrac{d}{d\varphi}\left(\dfrac{\beta'}{\beta}\right)=\dfrac{d}{d\varphi}\left(\dfrac{\bar{\beta}'}{\bar{\beta}}\right). \end{cases} \tag{19}$$

In the following section it will be shown that, although the condition (18) is strongly conservative against finger buckling, by means of the finger geometries verifying it (and that are stable) it is possible to realize a quite wide set of finger closure sequences.

3 ANTHROPOMORPHIC FINGER CLOSURE

For the two cases $\Phi_i=\pi/2$ and $\Phi_i=2\pi/3$ in Figure 5-a) and b) the curves of the ratio $\bar{\beta}_i/\beta_i$ as function of φ_i are reported. These curves have been obtained with values of the shape parameters belonging to the stability regions of fig 4. Inspection of diagrams of fig. 5 reveals that:

- All the curves have a vertical asymptote at $\varphi_i=\Phi_i$ because the non-dimensional arm β_i tends to zero as the angle φ_i tends to the maximum value Φ_i. This make unattainable the condition of maximum closure of the phalanxes, a property that has to be taken in account when the angle Φ_i has to be chosen based on the finger functional specifications.
- The mean slope of the curves is increasing with ε_i. The slope $\dot{\rho}_i$ of a curve is initially decreasing with φ_i until the minimum value $\dot{\rho}_{i\min}$ is reached in the characteristic point having coordinate $(\bar{\varphi}_i,\bar{\rho}_i)$. From this minimum point the slope increases monotonically until it diverges.
- Due to the presence of a minimum point for the slope, all the curves follow a quasi-linear trend in a range of φ_i values that is approximately centered on $\varphi_i=\bar{\varphi}_i$. The higher ε_i is and the smaller $\varepsilon_i^{(e)}$ is the wider this range of φ_i values is.
- Finally, the minimum slope $\dot{\rho}_{i\min}$ is a decreasing function of ε_i.

Since the curves of fig. 5 follows a sigmoidal trend, by them it is not possible to identify by a direct method the optimal geometry of the finger joints able to achieve a given closure sequence. For this reason, it is preferable to substitute the curves of fig. 5 a) and b) by the approximating straight lines that are tangent to the curves in their characteristic point $(\bar{\varphi}_i,\bar{\rho}_i)$. These straight lines are fully identified in terms of initial offsets $\hat{\rho}_i$ and slopes $\dot{\rho}_{i\min}$ listed in Tab. I and II as function of ε_i. and $\varepsilon_i^{(e)}$. This approximation of the non-dimensional arm ratios $\bar{\beta}_i/\beta_i$ is equivalent to approximating the corresponding sigmoidal curves of the ratios $r_i=\alpha_i\cdot(\bar{\beta}_i/\beta_i)$ by straight lines having slope equal to $\alpha_i\,\dot{\rho}_{i\min}$ and initial offset $\hat{r}_i=\alpha_i\,\hat{\rho}_i$.

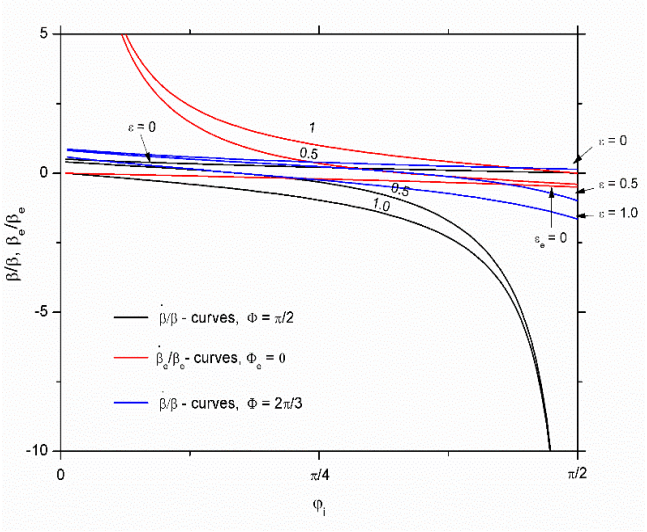

Figure 3 Diagram of logarithmic derivative $\bar{\beta}_i'/\bar{\beta}_i$ and β_i'/β_i as function of φ_i.

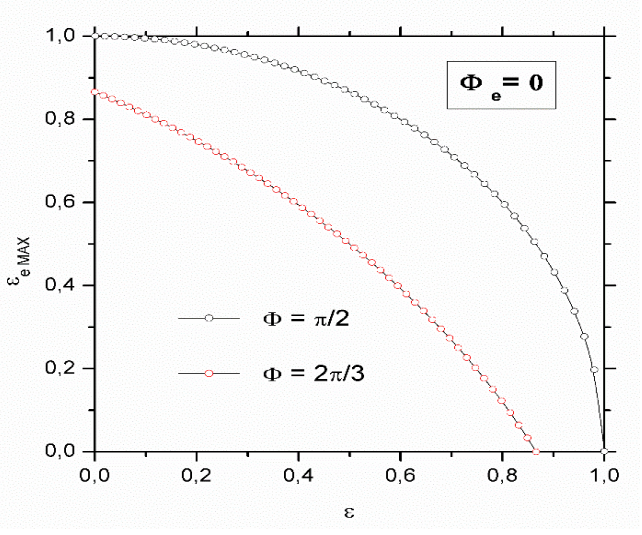

Figure 4 Diagram of the limit value $\bar{\varepsilon}_{\lim}$ as function of ε_i.

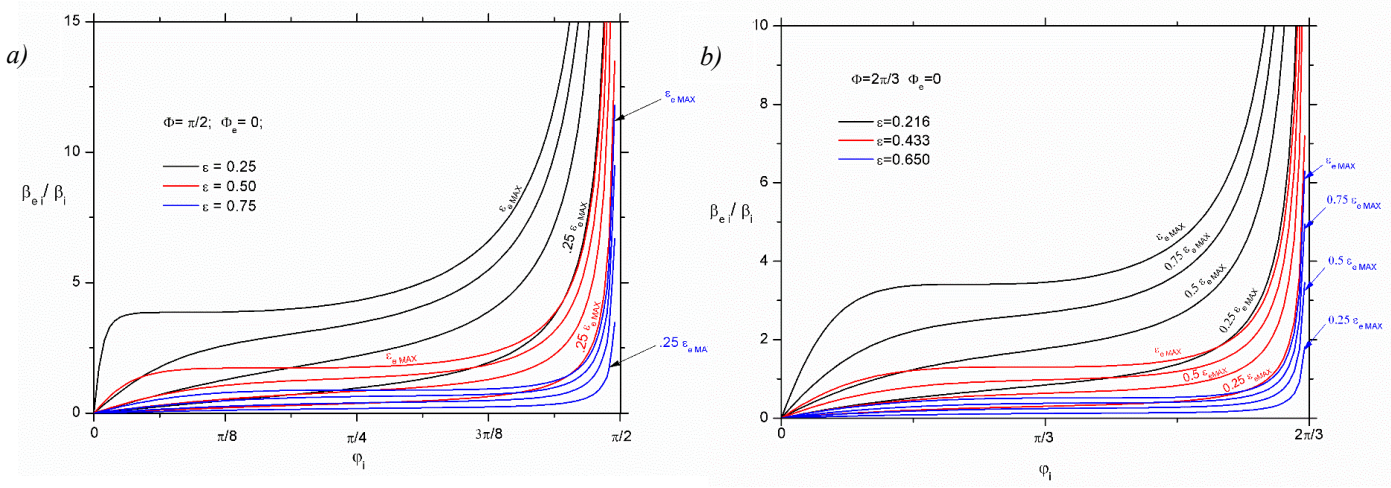

Figure 5 Diagrams of the non-dimensional arm-ratios $\rho_i = \overline{\beta}_i / \beta_i$ as function of φ_i : *a)* $\Phi = \pi/2$, *b)* $\Phi = 2\pi/3$.

By the data of Table I and II it is possible to carry out the preliminary design of a finger device having a closure sequence very similar to the one of a human finger. In other words, the closure will occurs by means of relative rotations taking place at first exclusively between the metacarpal and proximal phalanxes, then between the medial and proximal phalanxes and lastly between the medial and distal ones. To this aim, the shape ratios ε_i, $\overline{\varepsilon}_i$ and the parameters α_i have to be chosen such that the following conditions for the initial off-sets $\hat{r}_i$ and the abscissae's $r_{\Phi i}$ of fig. 6 are verified:

$$r_{\Phi 2} = \alpha_1 \left(\hat{\rho}_1 + \Phi_1 \dot{\rho}_{1\min} \right) < \alpha_2 \hat{\rho}_2 = \hat{r}_2$$
$$r_{\Phi 2} = \alpha_2 \left(\hat{\rho}_2 + \Phi_2 \dot{\rho}_{2\min} \right) < \alpha_3 \hat{\rho}_3 = \hat{r}_3. \qquad (20)$$

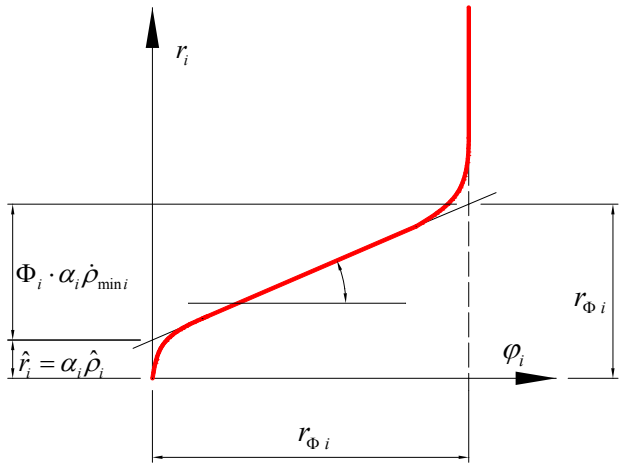

Figure 6 Diagram of the arm-ratio $r_i = \alpha_i \cdot \left(\overline{\beta}_i / \beta_i \right)$ as function of φ_i .

Table I - Initial offsets and slopes - $\Phi = \pi/2$

	$\overline{\varepsilon}$	$\dot{\rho}_{i\min}$	$\hat{\rho}_i$
ε = 0,25	0,242	1,149	0,026
$\overline{\varepsilon}_{\lim}$ = 0,968	0,484	2,210	0,441
	0,726	1,931	1,892
	0,968	0,000	3,861
ε = 0,50	0,216	0,400	0,055
$\overline{\varepsilon}_{\lim}$ = 0,866	0,433	0,674	0,310
	0,649	0,547	0,916
	0,866	0,000	1,730
ε = 0,75	0,165	0,132	0,072
$\overline{\varepsilon}_{\lim}$ = 0,661	0,331	0,197	0,236
	0,496	0,152	0,517
	0,661	0,000	0,881

Table II - Initial offsets and slopes - $\Phi = 2\pi/3$

	$\overline{\varepsilon}$	$\dot{\rho}_{i\min}$	$\hat{\rho}_i$
ε = 0,22	0,184	0,591	0,223
$\overline{\varepsilon}_{\lim}$ = 0,737	0,369	0,876	0,856
	0,553	0,677	1,973
	0,737	0,000	3,410
ε = 0,43	0,141	0,156	0,138
$\overline{\varepsilon}_{\lim}$ = 0,564	0,282	0,222	0,401
	0,423	0,169	0,799
	0,564	0,000	1,302
ε = 0,65	0,084	0,034	0,083
$\overline{\varepsilon}_{\lim}$ = 0,334	0,167	0,046	0,197
	0,251	0,034	0,342
	0,334	0,000	0,514

3.1 A FINGER CASE STUDY

In the following the results of some numerical simulations carried out for a finger whose joints verify the conditions (12), (18) and (20) are presented; this in order to give evidence to the design criteria proposed in the previous sections. Geometrical details of the analyzed device are listed in fig. 7. In the same figure the deformed configurations of the finger for several values of the displacement u imposed to the free end of the flexural tendon are shown. In the diagrams of fig. 8 a) and b) the relative rotations φ_i and the traction force of the flexor tendon, respectively, are reported as function of u.

Figures 7 and 8 show that:

- the geometry adopted for the joints is able to generate an anthropomorphic closure sequence;
- in the finger equilibrium path, buckling phenomena are absent.

In the diagram of fig. 8 a) sudden slope changes are observable. This is because the non-dimensional arm ratios ρ_i have a vertical asymptote at $\varphi_i = \Phi_i$. As far as this aspect is concerned, it must be remembered that during the closure for the finger equilibrium, (see eq. (11)), the arm ratios r_i of the three finger joints have to be equal. When at the joint i the arm ratio r_i reaches the asymptotic branch of the its curve $r_i - \varphi_i$, only very small increments of the relative rotation φ_i can occur for a given increment of r_i. Starting from this situation, further increments of the displacement u are essentially due to changes of the shortening Δz_j that occur at the other joints where the corresponding relative rotations φ_j start to increase more rapidly. The asymptotic branches of the $r_i - \varphi_i$ curves have an analogous effect also on the elongation Δl of the spring and, as a consequence, on the tendon traction $f = k\Delta l\left(\bar{b}_i / b_i\right)$. When the r_i asymptote is approached at the joint i, the corresponding local elongation Δl_i practically stops increasing while the local elongations at the other finger joints start increase more quickly for further fixed increments of the displacement applied to the flexural tendon end. This generates the sudden stiffness changes that are observable in the diagram of fig. 8 b).

4 CONCLUSIONS

The analysis of the equilibrium of an under-actuated finger was carried out following an energetic approach and has allowed identifying some preliminary design criteria for the regularity of the finger motion and for achieving an anthropomorphic closure sequence. Furthermore, a sufficient condition for the stability of the finger equilibrium has been also derived. A validation study has been carried out analyzing numerically the behavior of a finger designed according to the proposed criteria.

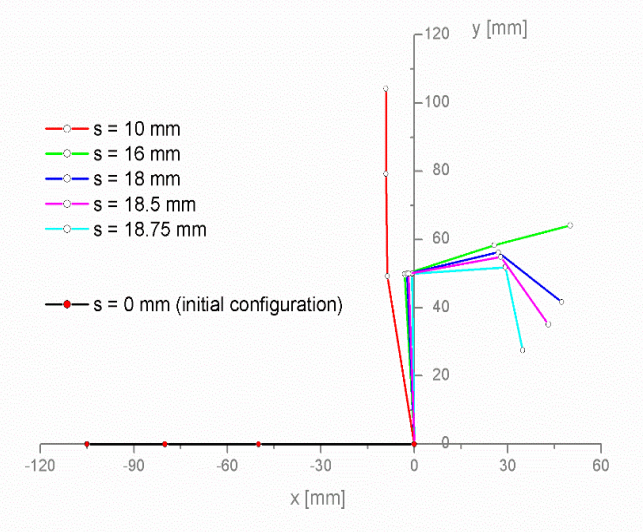

Figure 7 Deformed configurations of the examined finger device.

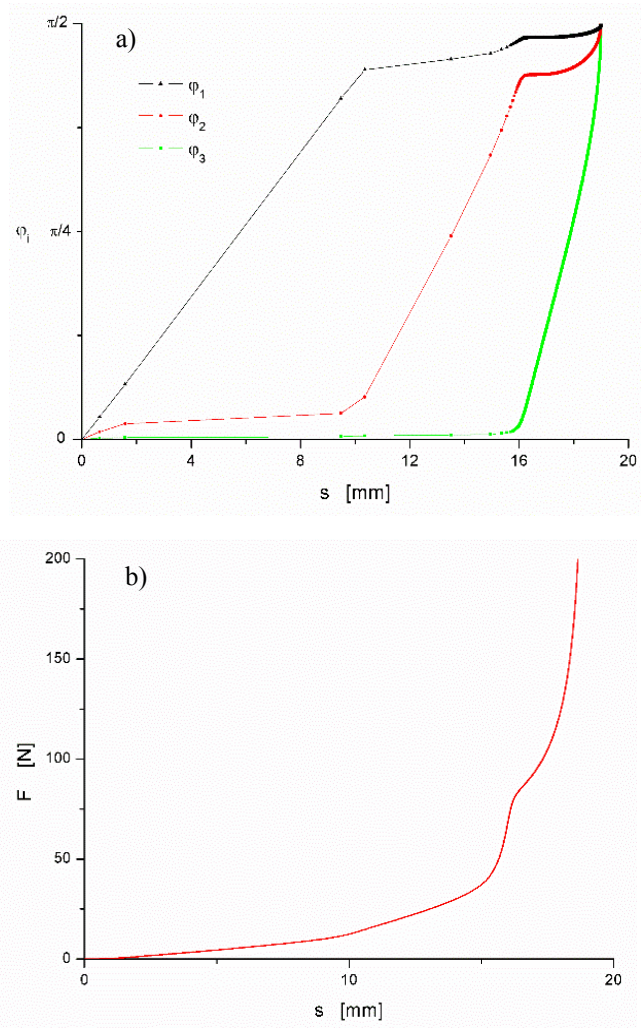

Figure 8 Diagrams of the relative rotations (a) and of the flexural tendon traction (b).

The obtained results are encouraging and justify further experimental analysis to be carried out on finger prototypes. Further investigations will consist in:

- analyzing experimentally and by numerical simulations the grasping capability of fingers designed according to the proposed criteria;
- studying the effect of this kind of fingers on the adaptive properties of an under-actuated mechanical hand;
- checking the finger closing sequence by adopting tendon laws of motion computed by means of the techniques proposed in [17, 18].

REFERENCES

[1] Hirose S., Umetani Y., The development of soft gripper for versatile robot hand. *Mechanism and Machine Theory*, Vol. 13, pp. 351-359, 1978.

[2] Townsend W., The Barret Hand grasper - programmably flexible part handling and assembly. *Industrial Robot: An International Journal*, Vol. 27, No. 3, pp. 181-188, 2000.

[3] Birglen L., Kragten G.A., Herder J.L., EDs., Underactuated Grasping. *Special issue in the Journal of Mechanical Sciences*, 2010.

[4] Kaneko M., Higashimori M., Takenaka R., Namiki A., Ishikawa M., The 100G capturing robot - too fast to see. *IEEE/ASME Transaction on Mechantronics*, Vol. 8, pp. 37-44, 2003.

[5] Laliberté T., Birglen L., Gosselin C., Underactuation in robotic grasping hands. *Machine Intelligence & Robotic Control*, Vol. 4, No. 3, pp. 1-11, 2002.

[6] Doria M., Birglen L., Design of an underactuated compliant gripper for surgery using nitinol. *Journal of Medical Devices*, Vol. 3, No. 1, 2009.

[7] Penta F., Rossi C., Savino S., An underactuated finger for a robotic hand. *International Journal of Mech. and Control*, Vol. 15, No. 2, pp. 63-68, 2014.

[8] Zottola M., Ceccarelli M., Underactuated finger mechanism for LARM hand. *Advances on Theory and Practice of Robots and Manipulators*, Springer International Publishing, pp. 283-291, 2014.

[9] Nelson C.A., Dessauw E., Saiter J.M., Benzohra, M., Design of a compliant underactuated robotic finger with coordinated stiffness. *Proc. of ASME 2013 International Design Engineering Technical Conf. and Computers and Information in Engineering Conf.*, American Society of Mechanical Engineers, 2013.

[10] Groenewegen M.W., Aguirre M.E., Herder J.L., Design of a partially compliant, three-phalanx underactuated prosthetic finger. *Proc. of ASME 2015 International Design Engineering Technical Conf. and Computers and Information in Engineering Conf.*, American Society of Mechanical Engineers, 2015.

[11] Rossi C., Savino S., An underactuated multi-finger grasping device. *International Journal of Advanced Robotic Systems*, Vol. 11, No. 1, 2014.

[12] Rossi C., Savino S., Niola V., Troncone S., A study of a robotic hand with tendon driven fingers. *Robotica*, Vol. 33, No. 5, pp. 1034-1048, 2015.

[13] Niola V., Rossi C., Savino S., Carbone G., Gaspareto A., Quaglia G., An underactuated mechanical hand prosthesys. *Proc. of 14th IFToMM World Congress*, Taipei, Taiwan, October 25-30, 2015, doi: 10.6567/IFToMM.14TH.WC.PS13.005.

[14] Birglen L., Gosselin C.M., On the force capability of underactuated fingers. *Proc. of 2003 IEEE International Conference on Robotics & Automation* Taipei, Taiwan, September 14-19, 2003.

[15] Birglen L., Gosselin C.M., Geometric design of three-phalanx underactuated fingers. *Journal of Mechanical Design - Transactions of the ASME*, Vol. 128, pp. 356-364, 2006.

[16] Kragten G.A., Herder J.L., The ability of underactuated hands to grasp and hold objects. *Mechanism and Machine Theory*, Vol. 45, pp. 408-425, 2010.

[17] Niola V., Rossi C., Savino S., Strano S., Robot trajectory planning by points and tangents. *Proc. of 10th WSEAS Int. Conference on Robotics, Control and Manufacturing Technology*, Hangzhou, China, April 11-13, ISSN: 1790-5117 91, ISBN: 978-960-474-175-5, pp. 91-96, 2010.

[18] Rossi C., Savino S., Robot trajectory planning by assigning positions and tangential velocities. *Robotics and Computer Integrated Manufacturing*, Vol. 29, ISSN: 0736-5845, doi: 10.1016/j.rcim.2012.04.003, pp. 139-156, 2013.

[19] Carbone G., Rossi C., Savino S., Performance comparison between FEDERICA Hand and LARM Hand. *Int. Journal of Advanced Robotic Systems*, Vol. 12, 2015. ISSN: 17298806, DOI: 10.5772/60523.

[20] Penta F., Rossi C., Savino S., Gripping analysis of an underactuated finger. *Advances in intelligent systems and computing: Proc. of 24th Internation Workshop on Robotics in Alpe-Adria-Danube Region*, Bucharest, Romania, May 27-29, doi: 10.1007/978-3-319-21290-6, pp. 71-78, 2015.

[21] Niola V., Penta F., Rossi C., Savino, S., An underactuated mechanical hand: theoretical studies and prototyping. *International Journal of Mechanics and Control*, Vol. 16, No. 1, ISSN: 1590-8844, pp. 11-19, 2015.

[22] Niola V., Rossi C., Savino S., Carbone G., Gaspareto A., Quaglia G., An underactuated mechanical hand prosthesys. *Proc. of 14th IFToMM World Congress*, Taipei, Taiwan, October 25-30, doi: 10.6567/ IFToMM.14TH.WC.PS13.005, 2015.